

PROGRESS OF SuperKEKB

T. Miura[#], T. Abe, T. Adachi, K. Akai, M. Akemoto, A. Akiyama, D. Arakawa, Y. Arakida, Y. Arimoto, M. Arinaga, K. Ebihara, K. Egawa, A. Enomoto, J. W. Flanagan, S. Fukuda, H. Fukuma, Y. Funakoshi, K. Furukawa, T. Furuya, K. Hara, T. Higo, H. Hisamatsu, H. Honma, T. Honma, R. Ichimiya, N. Iida, H. Iinuma, H. Ikeda, M. Ikeda, T. Ishibashi, H. Ishii, M. Iwasaki, A. Kabe, T. Kageyama, H. Kaji, K. Kakihara, S. Kamada, T. Kamitani, S. Kanaeda, K. Kanazawa, H. Katagiri, S. Kato, S. Kazama, M. Kikuchi, T. Kobayashi, H. Koiso, Y. Kojima, M. Kurashina, K. Marutsuka, M. Masuzawa, S. Matsumoto, T. Matsumoto, H. Matsushita, S. Michizono, K. Mikawa, T. Mimashi, F. Miyahara, K. Mori, T. Mori, A. Morita, Y. Morita, H. Nakai, H. Nakajima, T. T. Nakamura, K. Nakanishi, K. Nakao, H. Nakayama, T. Natsui, M. Nishiwaki, J. Odagiri, Y. Ogawa, K. Ohmi, Y. Ohnishi, S. Ohsawa, Y. Ohsawa, N. Ohuchi, K. Oide, T. Oki, M. Ono, H. Sakai, Y. Sakamoto, S. Sasaki, M. Sato, M. Satoh, K. Shibata, T. Shidara, M. Shirai, A. Shirakawa, M. Suetake, Y. Suetsugu, R. Sugahara, H. Sugimoto, T. Suwada, S. Takasaki, T. Takatomi, T. Takenaka, Y. Takeuchi, M. Tanaka, M. Tawada, S. Terui, M. Tobiyama, N. Tokuda, K. Tsuchiya, X. Wang, K. Watanabe, H. Yamaoka, Y. Yano, K. Yokoyama, M. Yoshida, M. Yoshida, S. Yoshimoto, K. Yoshino, R. Zhang, D. Zhou, X. Zhou, Z. Zong, KEK, Ibaraki, Japan
 D. Satoh, Tokyo Inst. of Technology, Tokyo, Japan

Abstract

SuperKEKB is designed based on the ‘nano-beam scheme’ with the target luminosity of $8 \times 10^{35} \text{ cm}^{-2}\text{s}^{-1}$. The design of the interaction region (IR) with a very low β_y^* at the interaction point (IP) is discussed. The status of the installation and the injector commissioning of SuperKEKB is reported.

INTRODUCTION

The previous project KEKB was an e^-/e^+ collider that is used for physics experiments mainly conducted at the Y(4S) resonance. KEKB has the highest peak luminosity in the world, $2 \times 10^{34} \text{ cm}^{-2}\text{s}^{-1}$. KEKB has been in operation until 2010. Afterward, upgrading of KEKB has been initiated toward SuperKEKB. The target luminosity is $8 \times 10^{35} \text{ cm}^{-2}\text{s}^{-1}$, which is 40times higher than that of KEKB. The required integral luminosity is 50 ab^{-1} . For the upgrade, the KEKB tunnel is being reused, and the KEKB components are being reused as much as possible in SuperKEKB.

Luminosity mainly depends on three parameters: the beam currents (I), the beam-beam parameter (ξ_y), and the vertical beta function (β_y^*) at the interaction point (IP). For achieving 40 times higher luminosity than that of KEKB, the current I is doubled, the beam-beam parameter ξ_y is kept almost at the same level, and β_y^* is reduced to 1/20 of the KEKB value, based on the ‘nano-beam scheme’. Table 1 shows the SuperKEKB machine parameters. As the nano-beam collision scheme, beams collide at a large crossing angle, 83 mrad. Thus, the length of the overlap region of the two beams at the IP is expressed as σ_x^*/ϕ . For realization of the small β_y^* , low horizontal emittance ϵ_x and small β_x^* are necessary. The

value of β_y^* at the SuperKEKB is 0.3 mm.

As part of an additional design concept, beam energies are changed. The LER energy is increased for longer Touschek lifetime and mitigation of emittance growth owing to the intra-beam scattering. In HER, as the energy is decreased, emittance becomes lower and synchrotron radiation (SR) power decreases. For the low SR power, the KEKB beam chamber can be reused.

Table 1: SuperKEKB Machine Parameters

Parameters	units	LER	HER
Beam energy	GeV	4	7.007
Half crossing angle ϕ	mrad	41.5	
Num. of bunches		2500	
H emittance ϵ_x	nm	3.2	4.6
Emittance ratio	%	0.27	0.25
Beta functions β_x^*/β_y^*	mm	32/0.27	25/0.30
Beam currents I	A	3.6	2.6
Beam-beam param. ξ_y		0.088	0.081
Bunch length	mm	6.0	5.0
H beam size σ_x^*	μm	10	11
V beam size σ_y^*	nm	48	62
Luminosity	$\text{cm}^{-2}\text{s}^{-1}$	8×10^{35}	

The estimated beam lifetimes for both rings are ~ 6 min, obtained without the consideration of without beam-beam effect. An effect of the beam-beam interaction to the beam lifetime and other beam-beam related issue are discussed elsewhere [1]. Therefore, high bunch charge

[#]takako.miura@kek.jp

Content from this work may be used under the terms of the CC BY 3.0 licence (© 2015). Any distribution of this work must maintain attribution to the author(s), title of the work, publisher, and DOI.

injection beams with low emittance are required. The LINAC has been upgraded, and the positron damping ring (DR) has been constructed anew for SuperKEKB.

UPGRADE STATUS OF MAIN RINGS

Final Focus Superconducting Magnets

SuperKEKB is based on the nano-beam scheme. Final focus (FF) quadrupoles have to be located as close to the IP as possible, because beam size is strongly reduced to the nm scale. The quadrupole magnets are, therefore, located inside the Belle II solenoid fields of 1.5T.

Figure 1 shows the layout of the FF superconducting magnet. Pairs of QC1 and QC2 are FF doublets. The QC magnets are equipped with the corrector coils for multipoles (normal/skew dipoles, skew quad, normal/skew sextupoles, octupole). ES solenoids are compensation solenoids for canceling the Belle II solenoid field. QC1LP and QC1RP in the LER are located in a strong solenoid field, and space is limited. Thus, they do not have the magnetic yokes. The corrector coils are installed in the HER line for canceling the leakage fields from QC1LP and QC1RP. The FF magnets have been very carefully designed and fabricated to minimize the higher multipole fields which are crucially important for the wide dynamic aperture.

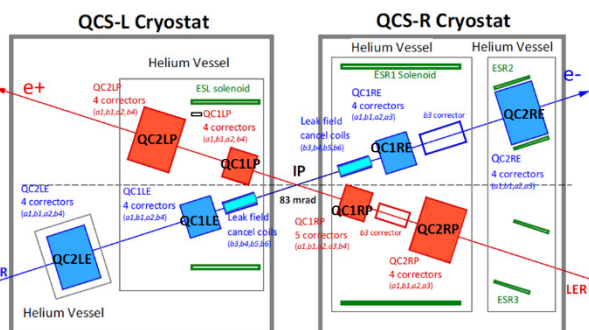


Figure 1: Layout of the FF superconducting magnets.

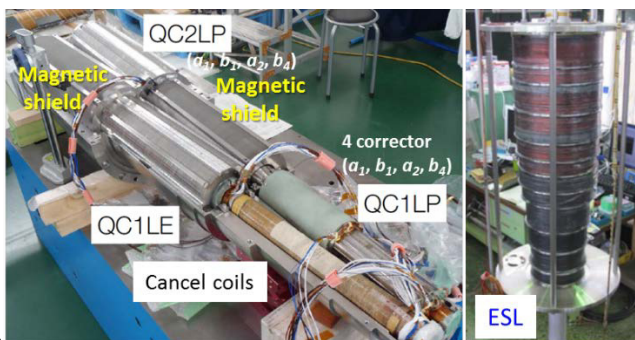


Figure 2: Picture of left side superconducting magnets.

Figure 2 shows a picture of left side superconducting magnets. Assemblies of all quadrupole magnets were completed. A cold test at the temperature of 4 K was performed for left side magnets. Satisfactory performance for beam operation was confirmed.

The Interaction Region

The natural chromaticity of SuperKEKB is higher than that of KEKB. Especially, the vertical chromaticity is high significantly. 80% of the chromaticity is induced by the FF. Horizontal and vertical local chromaticity corrections (LCC) are adopted for correcting large chromaticity near the FF in both rings as shown in Fig. 3.

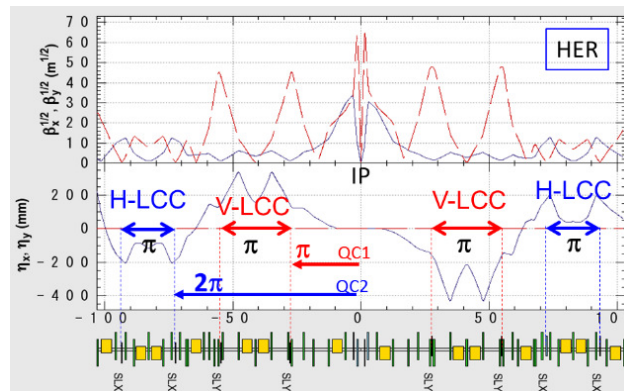


Figure 3: FF optics with local chromaticity corrections.

Since large crossing angle and LCC are adopted in SuperKEKB, the beam line of ~320 m around IR has been reconstructed completely. All components were dismantled in 2013. At present, almost all magnets have been installed as shown in Fig. 4.

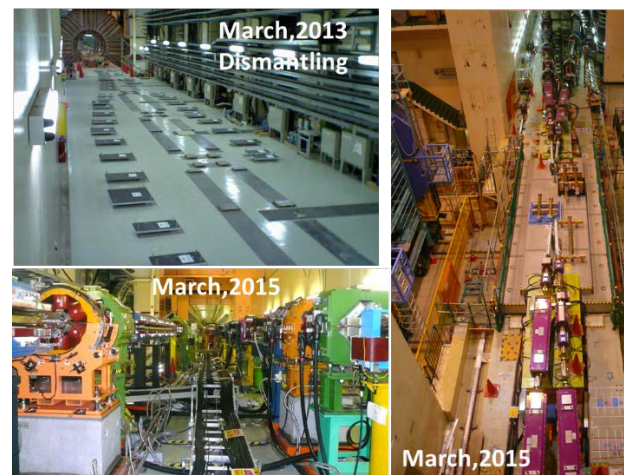


Figure 4: The beam line of ~320 m around IR has been reconstructed completely.

The Magnet System

For low horizontal emittance ϵ_x , the lattice was redesigned. The LER dipole magnets of 0.89 m in the arc were replaced with ones of 4 m, as shown in Fig. 5. In the case of HER, beta functions and dispersions were modified for making the emittance as small as possible because the dipole magnets in the KEKB HER are sufficiently long.

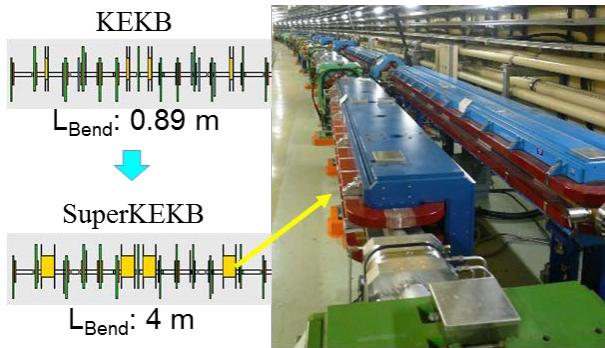


Figure 5: The LER dipole magnets of 0.89 m in the arc were replaced with ones of 4 m for low ϵ_x .

Figure 6 shows the wiggler magnets. Wiggler magnets have been installed in both rings for shortening of radiation damping time and reducing the emittance. In LER, wiggler cycles were shortened for small dispersion.

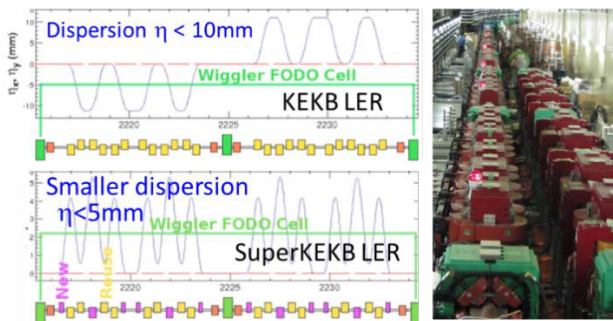


Figure 6: Wiggler magnets have been installed in the both rings. Wiggler cycle was shortened in LER.

Most of the magnets have already been installed. Integrated testing with power supply is in underway. The precise alignment work of magnets will be initiated soon.

The Vacuum System

Effects of the electron cloud in the LER positron ring are more serious than at KEKB. Various countermeasures for preventing emittance growth owing to head-tail instability are necessary. Table 2 shows the vacuum chambers installed in each section as the countermeasures.

In LER, almost all chambers were replaced with aluminium antechambers with TiN coating as shown in Fig. 7. Specifically, in the dipole magnet section, a grooved type antechamber with TiN coating is employed. In the wiggler section, an antechamber of copper with clearing electrode is employed, as shown in Fig. 8. Suppression rates of electron cloud are 1/5 with the antechambers, 1/50 with the solenoids, 1/4 with the grooves, and 1/100 with electrodes. TiN coating is 3/5 for Cu and 1/50 for Al. The TiN coating is indispensable for Al chamber because Al has high emission rate of secondary electrons. After TiN coating, the emission rate of secondary electrons is the same for Al and Cu. As of

this date, almost all beam pipes in LER have been already replaced with new ones.

Table 2: Vacuum Chambers in LER

Section	Vacuum chambers
Drift	Antechamber(Al) + TiN coating + Solenoid
Q, Sx mag	Antechamber(Al) + TiN coating
Bend	Antechamber(Al) + Groove + TiN coating
Wiggler	Antechamber(Cu) + Clearing electrode

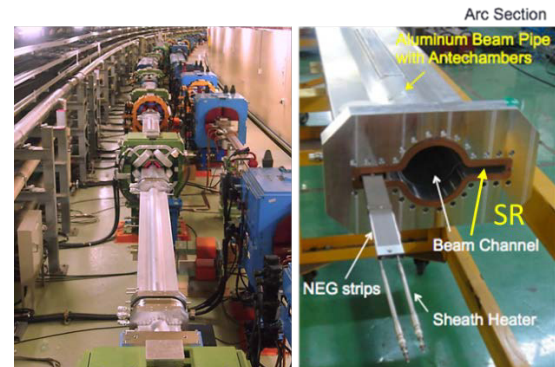


Figure 7: Aluminium antechamber with TiN coating.

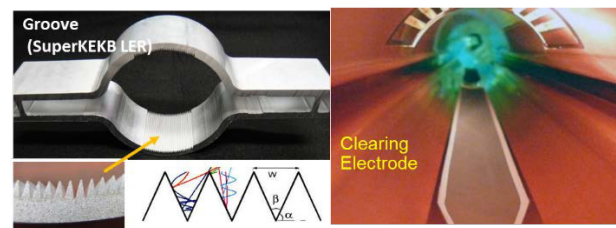


Figure 8: Groove-type antechamber (left) and antechamber with a clearing electrode (right).

UPGRADE OF THE LINAC

Table 3 shows the LINAC parameters. The requirements on the injection beam are: electrons of 5 nC/bunch and positrons of 4 nC/bunch, with low emittance ($\gamma\beta\epsilon_y$ below 20 mm-mrad). Positron capture section has been upgraded for four times higher positron yields compared with KEKB, and low emittance is realized by DR. The photo-cathode RF gun, which yields high bunch charge and low emittance, is being developed. This is a challenging work. The thermionic electron gun is also employed for producing a 10 nC beam of primary electrons for positron production, and it is located above the RF-gun. Two-bunch injection is performed for one pulse at the 50 Hz repetition rate. Figure 9 shows the layout and beam energy patterns of the LINAC. The LINAC serves as an injector for four rings (LER, HER, PF and PF-AR of light sources). Beam modes are switched in pulse-to-pulse for 5 rings including the DR.

Any distribution of this work must maintain attribution to the author(s), title of the work, publisher, and DOI.

Downstream of the DR, the acceleration energy depends on the beam mode. Therefore, pulsed quads and pulsed steering magnets will be installed for optimizing the optics for different beam energies and for simplifying the beam handling. For low emittance preservation, local and global alignment error tolerance values of 0.1 mm rms and 0.3 mm rms, respectively, are required [2].

Beam commissioning [3] has been performed during the upgrading. The status of the commissioning is reported as well.

Table 3: KEKB/SuperKEKB LINAC Parameters

Parameters	Positron	Electron
Beam Energy [GeV]	3.5 / 4.0	8.0 / 7.0
Bunch charge [nC]	1* / 4*	1 / 5
Emittance $\gamma\beta\epsilon_y$ [mm-mrad]	2100 / 20	100 / 20
Energy spread [%]	0.125 / 0.1	0.125 / 0.1
Number of bunch	2 / 2	2 / 2

(*) bunch charge of primary electron = 10 nC

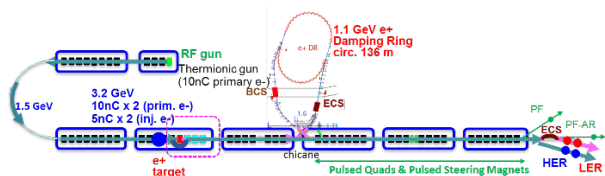


Figure 9: Layout of injector LINAC.

The Photocathode RF Gun System

A photocathode quasi-traveling wave side couple RF gun [4] was installed as a low-emittance electron-beam source in September of 2013, as shown in Fig. 10. This RF gun has a strong focusing force owing to accelerating field. Thus, it can generate electron beams with up to 10 nC charge. For 5nC/bunch, 5 mm-mrad normalized emittance is expected from simulations. For a photocathode, an Ir₃Ce cathode is employed. It has a long lifetime and its quantum efficiency is 10⁻⁴. The laser's incident angle is 60degrees relative the cathode surface. An Yb:YAG laser has been employed as a laser system.

Commissioning of the Photocathode RF Gun

The laser condition was 2 bunch×25 Hz. The RF gun acceleration voltage was limited to 6.5 MV by breakdown (design: 13.5 MV). Figure 11 shows the bunch charge immediately at the exit from the RF gun. At the beginning, the bunch charge was limited by the thermal effect. After the Yb:YAG thin-disk cooling was improved[5], the bunch charge of 4 nC has been maintained for a week. The laser power increased and the stability also improved.

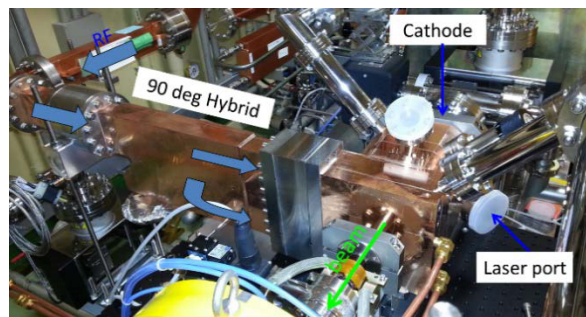


Figure 10: Photo-cathode Quasi-traveling wave RF gun.

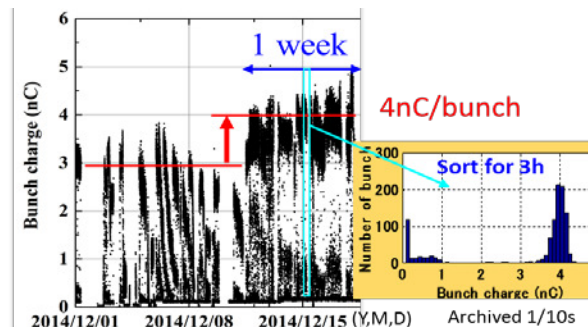


Figure 11: The bunch charge at the RF gun exit.

Emittance measurement was performed with quads scan. The beam current was 3 nC at the screen. The beam size was measured shot-by-shot by using a camera. The measured normalized emittance was 49 mm-mrad in the horizontal and 26 mm-mrad in the vertical directions. Emittance in the horizontal direction was higher than that in the vertical direction, which was caused by the laser's incidence angle. As a result, high acceleration voltage of RF gun is required for small emittance.

The Positron Capture Section

The positron capture section has been reconstructed completely for achieving the positron yield fourfold. Figure 12 shows the new positron capture section. It was installed in May 2014. The capture section consists of a flux concentrator (FC), a bridge coil, and six large-aperture S-band acceleration structures (LASs) covered by a DC solenoid. The FC is employed for large energy acceptance, and LASs are employed for large transverse acceptance. A hole ($\phi=2$ mm) for low emittance electron beam is on axis. The positron target is off axis. The orbits of the electron beam and of the primary electron beam for positron production are switched by using two pulse steering magnets upstream of the target.

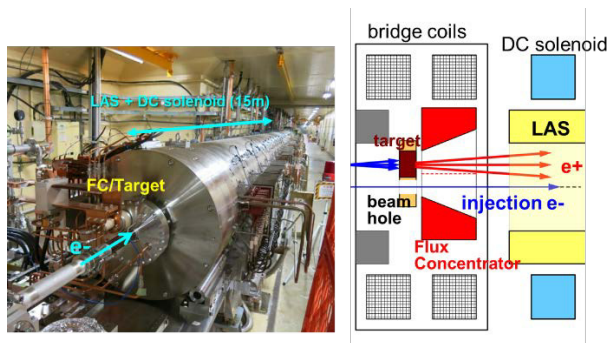


Figure 12: Photo of positron capture section (left) and schematic drawing around the positron target (right).

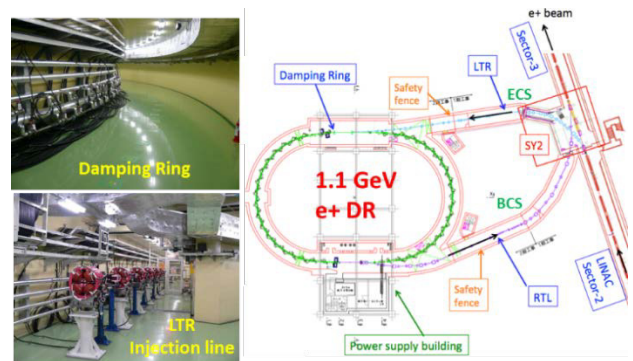


Figure 14: The 1.1 GeV positron damping ring.

Commissioning of Positron Capture Section

First positron commissioning was performed one month after the installation. Operation conditions of the FC current, the DC solenoid current, and the acceleration field of the LAS were not fulfilled at that time. The charge of primary electrons was 0.6 nC. The positron yield was 30% at the end of the capture section, and 20% at the end of Sector 2, as shown in Fig. 13. At the DR entrance, positron yield above 40% is necessary. Commissioning under condition of design parameters will start during October of 2015. From the simulations results, we expect a twofold higher positron yield.

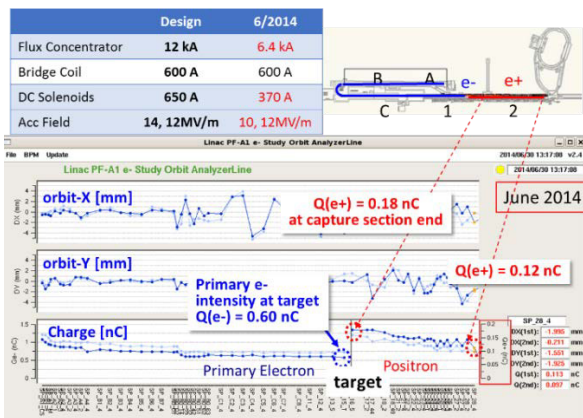


Figure 13: First result of positron beam commissioning.

THE POSITRON DAMPING RING

Construction of the DR tunnel was completed in March 2013. Figure 14 shows the 1.1 GeV positron DR. 'Reverse-bend FODO lattice' is employed as the DR normal cell. The features are:

- Shorter damping time (10.8 ms).
- Large momentum aperture (1.5%).
- Low momentum compaction (0.0144).

Emittance is damped from 1400 nm to 43 nm in 40 ms. As a current status, the installation of magnets in transport lines between LINAC and DR has almost been completed. The installation of magnets in ring will start during June of 2015.

SCHEDULE

The SuperKEKB commissioning will be performed in three stages: Phase 1, Phase 2, and Phase 3.

The first beam commissioning Phase 1 will start early next year. Vacuum scrubbing and basic machine tuning will be performed at that time. A 1 nC/bunch injection beam is required. Low emittance injection beam is not necessary.

Phase 2 is scheduled to start in the middle of 2017. The FF magnets and Belle II detector, except for a vertex detector, will be installed before Phase 2. Collision experiment is planned, and luminosity is expected to be the same as that of KEKB's design. Low emittance and 2 nC/bunch injection beam is required. DR beam commissioning, therefore, will start before Phase 2. Top-up injection with pulse-to-pulse mode switching is also necessary during this phase.

Phase 3 will start during October 2018. This is the start of the full current and full Belle II operation. At this time, low emittance and 4 nC/bunch injection beam will be required. We aim at a target luminosity of $8 \times 10^{35} \text{ cm}^{-2} \text{ s}^{-1}$.

REFERENCES

- [1] D. Zhou et al., "Interplay of Beam-Beam, Lattice Nonlinearity, and Space Charge Effects in the SuperKEKB Collider", WEYB3, IPAC'15, Richmond, VA, USA, May 2015.
- [2] S. Kazama et al., "Emittance Preservation in SuperKEKB Injector", MOPWA053, IPAC'15, Richmond, VA, USA, May 2015.
- [3] M. Satoh et al., "Commissioning of SuperKEKB Injector Linac", TUPTY008, IPAC'15, Richmond, VA, USA, May 2015.
- [4] T. Natsui et al., "Quasi-Traveling Wave RF Gun and Beam Commissioning for SuperKEKB", TUPJE003, IPAC'15, Richmond, VA, USA, May 2015.
- [5] R. Zhang et al., "Improvements of the Laser System for RF-Gun at SuperKEKB Injector", TUPWA071, IPAC'15, Richmond, VA, USA, May 2015.